OATAO
Open Archive Toulouse Archive Ouverte

Open Archive Toulouse Archive Ouverte (OATAO)

OATAO is an open access repository that collects the work of Toulouse researchers and makes it freely available over the web where possible.

This is an author-deposited version published in: http://oatao.univ-toulouse.fr/
Eprints ID : 3010

To link to this article :

URL: http://dx.doi.org/10.1016/S0013-4686(02)00688-6

Electrochemical preparation of peroxodisulfuric acid using boron doped diamond thin film electrodes

K. Serrano [a,*], P.A. Michaud [b], C. Comninellis [b,1], A. Savall [a,1]

[a] Laboratoire de Génie Chimique UMR 5503, Université Paul Sabatier, 118 route de Narbonne, 31062 Toulouse cedex 04, France
[b] Institute of Chemical Engineering, Swiss Federal Institute of Technology, CH-1015 Lausanne, Switzerland

Abstract

We have investigated the electrochemical oxidation of sulfuric acid on boron-doped synthetic diamond electrodes (BDD) obtained by HF CVD on p-Si. The results have shown that high current efficiency for sulfuric acid oxidation to peroxodisulfuric acid can be achieved in concentrated H_2SO_4 (> 2 M) at moderate temperatures (8–10 °C). The main side reaction is oxygen evolution. Small amounts of peroxomonosulfuric acid (Caro's acid) have also been detected. A reaction mechanism involving hydroxyl radicals, HSO_4^- and undissociated H_2SO_4 has been proposed. According to this mechanism electrogenerated hydroxyl radicals at the BDD anode react with HSO_4^- and H_2SO_4 giving peroxodisulfate.
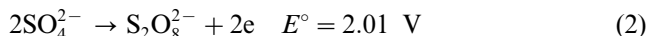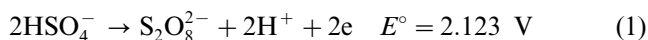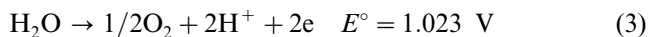
1. Introduction

The electrolysis of sulfuric acid solution could allow, in certain conditions, the electrosynthesis of persulfuric acid $H_2S_2O_8$. Persulfuric acid is widely used as oxidant in many applications. In wastewater treatment it is used for cyanides removal of effluents. Other applications concern dyes oxidation, fibres whitening, promotion for radical polymerization, total organic compound measurements... [1]. Persulfuric acid is an important intermediate product in the electrochemical production of hydrogen peroxide [1–3].

The $S_2O_8^{2-}$ ions are formed from the oxidation of SO_4^{2-} and HSO_4^- species at very high potentials:

$$2HSO_4^- \rightarrow S_2O_8^{2-} + 2H^+ + 2e \quad E° = 2.123 \text{ V} \quad (1)$$
$$2SO_4^{2-} \rightarrow S_2O_8^{2-} + 2e \quad E° = 2.01 \text{ V} \quad (2)$$

The discharge of water could be a secondary reaction:

$$H_2O \rightarrow 1/2O_2 + 2H^+ + 2e \quad E° = 1.023 \text{ V} \quad (3)$$

The electrochemical production of peroxodisulfates strongly depends on the electrode material selected for the oxidation of sulfuric acid. The main criterion is the high overpotential value for oxygen evolution reaction provided by the anode material.

This study concerns the peroxodisulfate formation using as anode the synthetic diamond film electrodes. Diamond films electrodes show high overpotentials for both hydrogen and oxygen evolution in aqueous solutions. The electrochemical window at diamond electrodes is about 3 V large for a 1 mol l^{-1} sulfuric acid solution, and exhibits a low background current in the solvent stability domain [4–6]. It has been shown that only reactions involving simple electron transfer are active on diamond electrodes in the potential region of water stability. For reactions with more complex mechanisms, oxidation can take place on diamond electrodes only in the potential region of supporting electrolyte or/and water discharge [7].

The diamond electrodes have been also successfully used for the anodic oxidation of cyanide and the cathodic recovery of heavy metals [8].

Actual electrochemical processes for persulfates synthesis use noble metal coated anodes (platinized titanium, tantalum or niobium). The anodic formation

of persulfates has been studied [9–16] but the reaction mechanism is still unsettled. Two contradictions of reaction paths on platinum electrode were reported in literature. Some authors reported that formation of $S_2O_8^{2-}$ ions result from direct oxidation of HSO_4^- [9] or SO_4^{2-} [10] or simultaneous by HSO_4^- and SO_4^{2-} [11] according to equations (1) and (2). Alternatively to this mechanism, others suggest a primary formation of radicals which is stemming from water discharge [12,13] followed by a reaction with sulfate.

In most of these studies, one or some adsorption phenomena were shown to determine the kinetics of $S_2O_8^{2-}$ formation on platinum electrode. Elbs and Schönherr [14] observed a considerable rise of the current efficiency from 45 to 85% of persulfate formation after addition in the sulfuric acid solution of ammonium cations. They ascribed the effect of various cations on the current efficiency to an unspecified catalytic effect. According to Smit and Hoogland [10] the coverage of the surface of platinum by oxygen is increasingly replaced by patches of adsorbed SO_4^{2-} on which $S_2O_8^{2-}$ formation proceeds instead of oxygen evolution. Another explanation is given by Kasatkin and Rakov [15]: these additives block up the active centers and favor recombination of atomic oxygen which reacts with sulfate species. According to Frumkin [16], oxygen is chemisorbed resulting in a discontinuous rise of oxygen overvoltage.

The aim of this study, following a previous paper [17], is to propose the reaction path of the $S_2O_8^{2-}$ formation on synthetic diamond film electrodes in sulfuric acidic medium.

The first part is the electrochemical study carried out by cyclic voltammetry. The second part concerns the preparation of persulfate by galvanostatic electrolysis. The influences of the temperature and the concentration of sulfuric acid are pointed out.

2. Experimental

Boron-doped diamond films, Diachem®, were synthesized by the hot filament chemical vapor deposition technique (HF CVD) on conducting p-Si substrate (0.1 Ω cm, Siltronix). The filament temperature ranged from 2440 to 2560 °C and the substrate one was kept at 830 °C. The reactive gas used was methane in an excess of dihydrogen (1% CH_4 in H_2). The doping gas was trimethylboron with a concentration of 3 ppm. The gas mixture was supplied to the reaction chamber, providing a 0.24 μm h^{-1} growth rate for the diamond layer. The diamond films were about 1 μm thick. This HF CVD process, produces columnar, randomly textured, polycrystalline films.

Electrochemical measurements were carried out in a conventional three-electrode cell using a computer controlled EG&G potentiostat model M 273. Diamond was used as working electrode, Hg/Hg_2SO_4, K_2SO_4 (sat) as a reference and Pt as counter electrode.

The oxidation of sulfuric acid is performed in a two compartments electrolytic flow cell under galvanostatic conditions (Fig. 1). Diamond is used as anode and zirconium as cathode. Both electrodes were disks (90 mm diameter) with a geometric area of 63 cm^2 each. The inter-electrode gap was 10 mm.

The set-up is illustrated in Fig. 2. The electrolytes (catholyte and anolyte) were stored in two 250 ml thermoregulated glass reservoirs (B1 and B2) and circulated through the electrolytic cell using two centrifugal pumps (P1 and P2). The flow rate of the electrochemical cell was 200 1 h^{-1}. The flow rate of electrolyte supply to the cell stored in the tanks B3 and B4 was 0.04 1 h^{-1}. The value of the current density used was 23 mA cm^{-2}. The electrolysis duration is 20 h. The peroxomonosulfuric acid and the hydrogen peroxide are simultaneously titrated by back titration with As(III) and Ce(IV).

The sum of peroxomonosulfuric acid, hydrogen peroxide and peroxodisulfuric acid is back titrated using Fe(II) and $KMnO_4$. The peroxodisulfuric acid is deduced from the two preceding results.

3. Results and discussion

The cyclic voltamgramm, Fig. 3, shows the cathodic part before (A) and after (B) the scan in the anodic part in a sulfuric acid solution (1 M). During the second cycle (B) a specie, formed during the anodic scan, is reduced at −1 V versus ref. This phenomenon is not observed in perchloric acid. This specie should be peroxodisulfate formed by oxidation of the sulfate ions during the first scan. In order to confirm the formation of peroxodisulfate in the anodic scan, an anodic polarization is holded at 2.4 V versus ref. (corresponding to a charge of 1.2 C) and immediately a cathodic scan is performed.
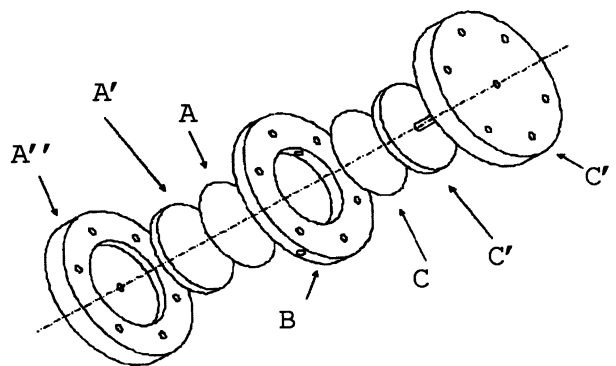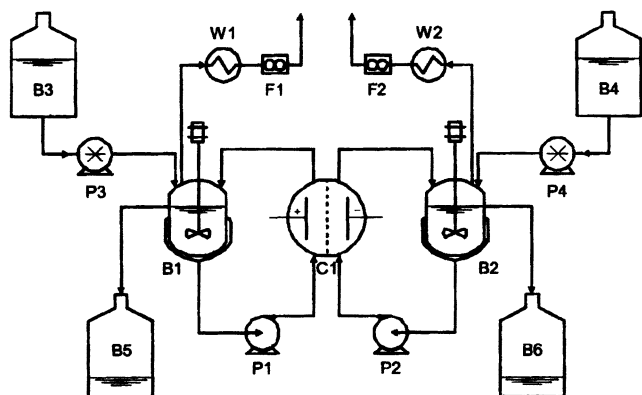
Fig. 2. Set up used for electrochemical oxidation of sulfuric acid on Si/diamond anodes. C1, electrochemical cell; B1 and B2, anodic and cathodic (respectively) thermoregulated tank (250 ml); B3 and B4 feed tank anodic and cathodic (10 l); B5 and B6, purge tank; P1 and P2, centrifugal pump feeding the anodic and cathodic compartment.
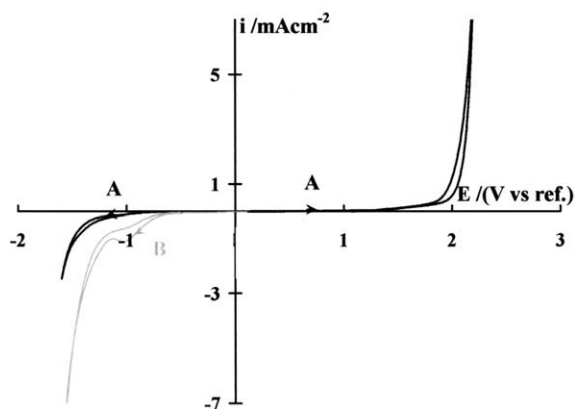

Fig. 3. Cyclic voltammogram of boron doped diamond electrode in sulfuric acid (1 mol dm^{-3}) [A] before and [B] after the scan in the anodic part. Scan rate = 50 mV s^{-1}, $T = 20$ °C; reference electrode, Hg/Hg$_2$SO$_4$/K$_2$SO$_4$ (sat); counter electrode, platinum.

Fig. 4 represents the plots obtained in perchloric and sulfuric acid, respectively. The lack of the cathodic wave after the anodic polarization in perchloric acid confirms that the cathodic wave is formed after oxidation of the sulfate ions. Besides, the cathodic wave observed at -1 V versus ref. increases after an addition of K$_2$S$_2$O$_8$ in the bulk, curve (c).

Thus the formation of the peroxodisulfuric acid coincides with the oxygen formation. The mechanism of anodic evolution of O$_2$ has been studied extensively at different electrodes in aqueous media [21,22]. The first step in the mechanism is the anodic discharge of H$_2$O to produce hydroxyl radicals (OH$^\bullet$) as indicated by eq (4):

$$H_2O \rightarrow OH^\bullet + H^+ + e \qquad (4)$$

In sulfuric acid solutions, sulfate anion, hydrogenosulfate anion and undissociated sulfuric acid coexist [23–26]. According to Librovich and Maiorov [23] the concentrations of hydrogenosulfate ([HSO$_4^-$]) and un-
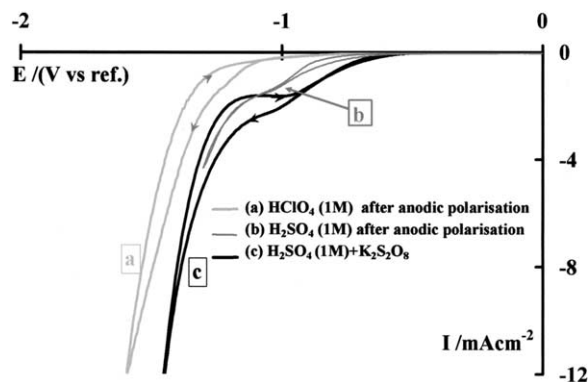

Fig. 4. I vs. E curve after an anodic polarization at $+2.4$ V vs ref. (charge = 1.2 C) of boron doped diamond electrode (a) in perchloric acid and (b) in sulfuric acid (1 mol dm^{-3}) (c) after addition of K$_2$S$_2$O$_8$ (4×10^{-2} M) in sulfuric acid. Scan rate = 50 mV s^{-1}, $T = 20$ °C, reference electrode, Hg/Hg$_2$SO$_4$/K$_2$SO$_4$ (sat); counter electrode, platinum.
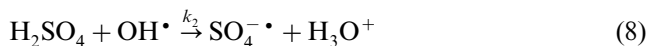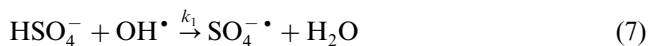
dissociated sulfuric acid ([H$_2$SO$_4$]) in mol dm^{-3} are given by:

$$[HSO_4^-] = 0.07663 + 0.7716C - 0.03052C^2 + 2.303$$
$$\times 10^{-3}C^3 \qquad (5)$$

$$[H_2SO_4] = 5.549 \times 10^{-3} - 0.03389C + 0.02862C^2$$
$$+ 4.984 \times 10^{-4}C^3 \qquad (6)$$

where C (mol dm^{-3}) is defined as: $C = [HSO_4^-] + [SO_4^{2-}] + [H_2SO_4]$, in which [H$_2SO_4$] represents the undissociated sulfuric acid. These equations are for $0 < C < 8$ mol dm^{-3} and $T = 25$ °C. Fig. 5 illustrates the concentrations of different species as a function of the concentration C.

According to refs [28–30], only HSO$_4^-$ and molecular H$_2$SO$_4$ react with OH$^\bullet$ radicals to form sulfate radicals, following reactions (7) and (8):

$$HSO_4^- + OH^\bullet \xrightarrow{k_1} SO_4^{-\bullet} + H_2O \qquad (7)$$

$$H_2SO_4 + OH^\bullet \xrightarrow{k_2} SO_4^{-\bullet} + H_3O^+ \qquad (8)$$

$$SO_4^{-\bullet} + SO_4^{-\bullet} \xrightarrow{k_3} S_2O_8^{2-} \qquad (9)$$

At the same time, a competitive reaction between the hydroxyl radicals may take place:

$$OH^{\bullet} + OH^{\bullet} \xrightarrow{k_4} O_2 + 2H^+ + 2e \qquad (10)$$
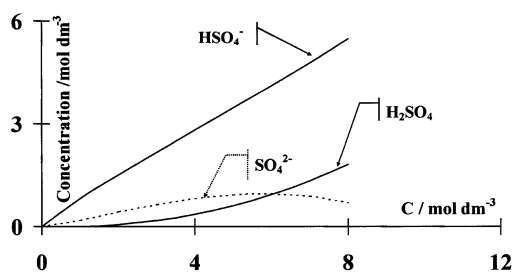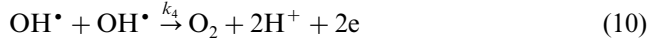
The values of the rate constants $k_{1\text{-}4}$ are reported in Table 1.

If we consider that the hydroxyl radicals are free and the concentration is constant in the reaction layer and according to steps 7 to 10, the rate of disappearance of the hydroxyl radicals is given by the following expression:

$$v = \frac{d[OH^{\bullet}]}{dt}$$

$$= k_1[HSO_4^-][OH^{\bullet}] + k_2[H_2SO_4][OH^{\bullet}] + k_4[OH^{\bullet}]^2 \qquad (11)$$

The current efficiency, η, is defined as the ratio between the number of electrons used for the sulfate radical formation and the total number of the electrons used.

$$\eta = \frac{k_1[HSO_4^-][OH^{\bullet}] + k_2[H_2SO_4][OH^{\bullet}]}{2k_4[OH^{\bullet}]^2 + k_1[HSO_4^-][OH^{\bullet}] + k_2[H_2SO_4][OH^{\bullet}]} \qquad (12.a)$$

The relation (Eq. (12.a)) could be linearized:

$$\frac{\eta}{1-\eta} \times \frac{1}{[HSO_4^-]}$$

$$= \frac{k_1}{2k_4[OH^{\bullet}]} + \frac{k_2}{2k_4[OH^{\bullet}]} \times \frac{[H_2SO_4]}{[HSO_4^-]} \qquad (12.b)$$

Galvanostatic electrolyses have been performed with regular samples which are taken at the input and output of the set-up. The variation of the concentration of peroxodisulfuric acid $[S_2O_8^{2-}]$ (mol m^{-3}), allows to calculate the experimental current efficiency η_{exp} expressed as:

$$\eta_{exp} = \frac{zF\Phi}{I}([S_2O_8^{2-}]_{outlet} - [S_2O_8^{2-}]_{inlet}) \qquad (13)$$

where z is the number of exchanged electrons (two electrons for 1 mol of $S_2O_8^{2-}$), F the Faradic constant (C mol^{-1}), Φ the flow rate of the electrochemical cell (m^3 s^{-1}), and I is the current (A).

Table 1
Values of the constant rate k_1, k_2, k_3 and k_4 of the sulfate radical at pH 1

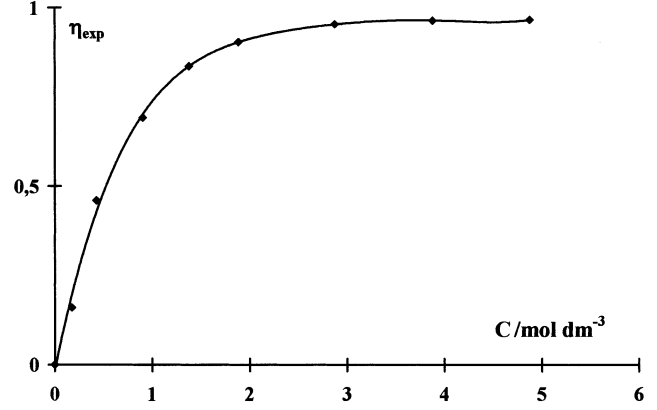|	
k_1 (dm^3 mol^{-1} s^{-1})	4.7×10^5** [28]; 3.5×10^5* [29]; 6.9×10^5* [30]
k_2 (dm^3 mol^{-1} s^{-1})	1.4×10^7** [28]
k_3 (dm^3 mol^{-1} s^{-1})	$(7.6 \pm 1)10^8$** [28]
k_4 (dm^3 mol^{-1} s^{-1})	1.1×10^{10}** [28]

*, $T = 25\ °C$ and **, $T = 20\ °C$ [28–30].

Fig. 6. Plot of η_{exp} vs. C on boron doped diamond electrode. Current density = 23 mA cm^{-2}, $T = 9\ °C$.

The influence of the concentration C on the experimental current efficiency at $T = 9\ °C$ is reported in Fig. 6. It appears two zones.
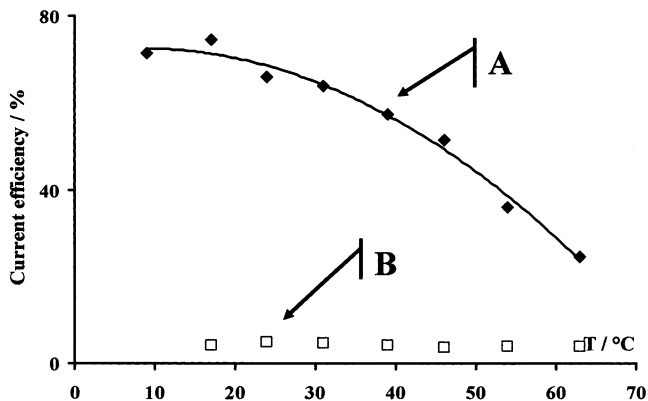
- For $C < 2$ M, the current efficiency increases with the concentration up to 90%.
- For $C > 2$ M, the current efficiency is constant to a maximum value of 95%.

It appears that in these experimental conditions of temperature (9 °C) and current density (23 mA cm^{-2}), the maximum current efficiency is obtained with $C > 2$ M. It is interesting to note that the maximum value of the current efficiency in this study is higher than those obtained in industrial electrosynthesis on platinum electrode (about 70–75%) [1,27].

The plot Fig. 7 checks the relation (Eq. (12.b)). The linear representation is in accordance with the reaction path of the peroxodisulfuric proposed in the set of reactions (7), (8), (10). The slope allows to calculate the average concentration of hydroxyl radicals in the reaction layer. Considering the rate constants given in Table 1, one obtains $[OH^{\bullet}] \approx 10^{-5}$ mol l^{-1}.

The plot reported in Fig. 8 evidences the influence of the temperature on the current efficiency of the peroxodisulfate production (curve A) in a sulfuric acid solution (1 M) by galvanostatic electrolysis ($i = 23$ mA
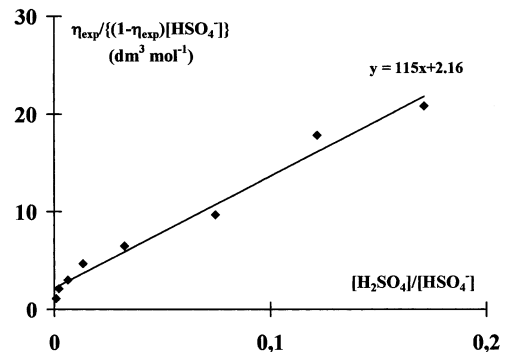
cm^{-2}). We can note that the current efficiency decreases with the temperature. At 65 °C, it falls down to 27%.

The persulfuric acid is unstable in aqueous solution, decomposing in dilute sulfuric acid solutions with liberation of oxygen according to reaction (14):

$$S_2O_8^{2-} + H_2O \rightarrow 2HSO_4^- + \tfrac{1}{2}O_2 \tag{14}$$
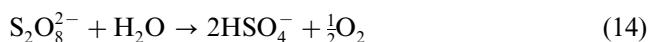
In more concentrated sulfuric acid solutions hydrogen peroxide rather than oxygen is formed (reactions (15) and (16)).

$$H_2S_2O_8 + H_2O \rightarrow H_2SO_5 + H_2SO_4 \tag{15}$$

$$H_2SO_5 + H_2O \rightarrow H_2O_2 + H_2SO_4 \tag{16}$$
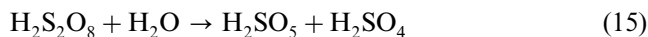
The formation of peroxomonosulfuric acid (H_2SO_5) in strongly acid peroxodisulfate solutions was observed by Caro [28]. Later work by Palme [29] showed that this acid is an intermediate in the decomposition of persulfuric acid in strongly acid solutions to form hydrogen peroxide.

The decomposition rate of potassium persulfate in solutions of various hydrogen ion concentrations was determined by Kolthoff and Miller [30] at 50 °C. They assumed that persulfate decomposes by two simultaneous reactions, one uncatalyzed and another catalyzed by hydrogen ions; the reaction rate is given by:

$$-d[S_2O_8^{2-}]/dt = k_1' [S_2O_8^{2-}] + k_2'[H^+][S_2O_8^{2-}] \tag{17}$$

$$-d[S_2O_8^{2-}]/dt = [S_2O_8^{2-}](k_1' + k_2'[H^+]) \tag{18}$$

with $k_0 = k_1' + k_2'[H^+]$.

The decrease of the current efficiency with the temperature can be explained by the increase of the constant rate of the decomposition of the persulfate [30], k_0.

Caro's acid is present in the bulk but the quantities are low (see Fig. 8, curve B), since Caro's acid (which is the product of the hydrolysis of $S_2O_8^{2-}$ (eq. 15)) is oxidized during the electrolysis following the reaction below:

$$H_2SO_5 + H_2O \rightarrow O_2 + H_2SO_4 + 2H^+ + 2e \tag{19}$$

According to Balej et al. [31], the oxidation rate of Caro's acid under common conditions of $S_2O_8^{2-}$ electrosynthesis is higher than the rate of the eventual formation of H_2SO_5. This is the reason why the concentration of Caro's acid does not increase with the temperature (Fig. 8).

References

[1] N. Ibl, H. Vogt, in: J.O.'M. Bockris, B.E. Conway, E. Yeager, R.E. White (Eds.), Comprehensive Treatise of Electrochemistry, vol. 2, Plenum Press, New York, 1981, p. 224.
[2] C. Oloman, A.P. Watkinson, Can. J. Chem. Eng. 54 (1976) 312.
[3] C. Comninellis, in: C.A.C. Sequeira (Ed.), Environmental Oriented Electrochemistry, Elsevier, Amsterdam, 1994.
[4] J.J. Carey, C.S. Christ, S.N. Lowery, US Patent 5399247 (1995).
[5] W. Haenni, H. Baumann, C. Comninellis, D. Gandini, P. Niedermann, A. Perret, N. Skinner, Diamond Relat. Mater. 7 (1998) 569.
[6] A. Perret, W. Haenni, P. Niedermann, H. Baumann, N. Skinner, C. Comninellis, D. Gandini, Proceedings of the International Symposium on Diamond Related Materials 5th, PV 97-32, 275, The Electrochemical Society Proceedings Series, Pennington, NJ, 1997.
[7] D. Gandini, P.A. Michaud, I. Duo, E. Mahè, W. Haenni, A. Perret, C. Comninellis, New Diamond Frontier Carbon Technol. 9 (1999) 303.
[8] A. Perret, W. Haenni, N. Skinner, X.-M. Tang, C. Comninellis, D. Gandini, B. Correa, G. Foti, Diamond Relat. Mater. 8 (1999) 820.
[9] W. Starck, Z. Phys. Chem. 29 (1899) 385.
[10] W. Smit, J.G. Hoogland, Electrochim. Acta 16 (1971) 1.
[11] W.D. Bancroft, Trans. Electrochem. Soc. 71 (1937) 159.
[12] J.W. Schultze, Ber. Bunsengens. Phys. Chem. 73 (1969) 483.
[13] F. Foerster, in: J.A. Barth (Ed.), Elektrochemie wässiger Lösungen, Leipzig, 1923.
[14] K. Elbs, O. Schönherr, Z. Elektrochem. 2 (1895) 245.
[15] E.V. Kasatkin, A.A. Rakov, Electrochim. Acta 10 (1965) 131.
[16] A. Frumkin, Electrochim. Acta 5 (1961) 265.
[17] P.-A. Michaud, E. Mahé, W. Haenni, A. Perret, C. Comninellis, Electrochem. Solid-State Lett. 3 (2) (2000) 77.
[18] J.P. Hoare, The Electrochemistry of Oxygen, Wiley, New York, 1968.
[19] J.O.'M. Bockris, J. Chem. Phys. 24 (1956) 817.
[20] S. Trasatti, J. Electroanal. Chem. 11 (1980) 125.
[21] P. Ruetschi, P. Delahay, J. Chem. Phys. 23 (1955) 556.
[22] J.E. Vitt, D.C. Johnson, J. Electrochem. Soc. 139 (3) (1992) 774.
[23] N.B. Librovich, V.D. Maiorov, Izv. Akad. Nauk SSSR Ser. Khim. 3 (1977) 684.

[24] P.Y. Jiang, Y. Katsumura, R. Nagaishi, M. Domae, K. Ishikawa, K. Ishigure, J. Chem. Soc. Faraday Trans. 88 (12) (1992) 1653.

[25] Y. Tang, R.P. Thorn, R.L. Mauldin, P.H. Wine, J. Photochem. Photobiol. A44 (3) (1988) 243.

[26] E. Heckel, A. Henglein, G. Beck, Ber. Bunsenges. Phys. Chem. 70 (1966) 149.

[27] J. Balej, M. Kaderavek, Collect. Czech. Chem. Commun. 44 (1979) 1510.

[28] H. Caro, Z. Angew. Chem. 845 (1898).

[29] H. Palme, Z. Anorg. Chem. 112 (1920) 97.

[30] I.M. Kolthoff, I.K. Miller, J. Am. Chem. Soc. 73 (1951) 3055.

[31] J. Balej, M. Thumova, M. Kaderavek, Collect. Czech. Chem. Commun. 45 (1980) 3254.